analytical chemistry

Article

pubs.acs.org/ac

In Vivo Noninvasive Monitoring of Glucose Concentration in Human Epidermis by Mid-Infrared Pulsed Photoacoustic Spectroscopy

Miguel A. Pleitez,[†] Tobias Lieblein,[†] Alexander Bauer,[†] Otto Hertzberg,[†] Hermann von Lilienfeld-Toal,[‡] and Werner Mäntele*[,†]

[†]Institut für Biophysik, Goethe-Universität Frankfurt, Max von Laue-Strasse 1, 60438 Frankfurt am Main, Germany

[‡]Elté Sensoric GmbH, 63571 Gelnhausen, Germany

ABSTRACT: The noninvasive determination of glucose in the interstitial layer of the human skin by mid-infrared spectroscopy is reported. The sensitivity for this measurement was obtained by combining the high pulse energy from an external cavity quantum cascade laser (EC-QCL) tunable in the infrared glucose fingerprint region (1000−1220 cm^{-1}) focused on the skin, with a detection of the absorbance process by photoacoustic spectroscopy in the ultrasound region performed by a gas cell coupled to the skin. This combination facilitates a quantitative measurement for concentrations of skin glucose in the range from <50 mg/dL to >300 mg/dL, which is the relevant range for the glucose monitoring in diabetes patients. Since the interstitial fluid glucose level is representative of the blood glucose level and follows it without significant delay (<10 min), this method could be applied to establish a noninvasive, painless glucose measurement procedure that is urgently awaited by diabetes patients. We report here the design of the photoacoustic experiments, the spectroscopy of glucose *in vivo*, and the calibration method for the quantitative determination of glucose in skin. Finally, a preliminary test with healthy volunteers and volunteers suffering from diabetes mellitus demonstrates the viability of a noninvasive glucose monitoring for patients based on the combination of infrared QCL and photoacoustic detection.

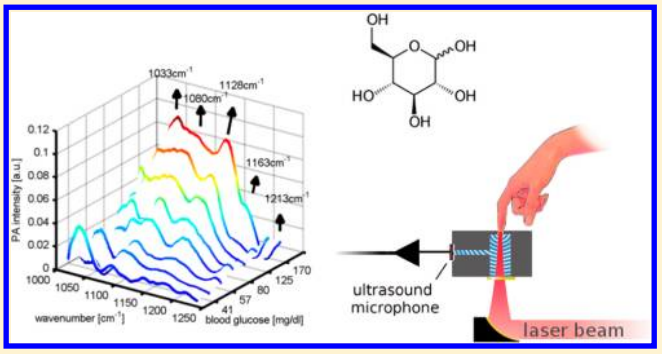

Diabetes mellitus concerns more than 346 million people worldwide, with increasing tendency. According to the World Health Organization (WHO), more than 80% of the diabetes-related deaths occur in low- and middle-income countries, making this disease a global challenge.[1] It is well understood that diagnosis and treatment require a regular or ideally continuous control of the glucose level in blood in order to optimize the treatment and to improve the quality of life of the patients. The established self-monitoring technique for blood glucose is based on enzyme reactions and amperometric detection. This procedure is painful because it requires the invasive extraction of a drop of blood from the patient by piercing the finger with a needle and costly because each measurement requires a new test strip. Ideally, the patient has to carry out these measurements several times a day. This invasive procedure, however, is well-established and selective because of the enzyme reaction used, although its precision (approximately ±20%) is limited.[2,3]

There are many attempts to develop alternative noninvasive procedures for the glucose measurement which, if practically applicable, should be of a sensitivity, selectivity, and precision at least comparable to the presently available invasive techniques. Some approaches are transdermal, such as the electric technique of skin impedance spectroscopy or the technique of reverse iontophoresis where interstitial fluid (ISF) is caused to diffuse to the skin surface and is measured with enzyme electrodes. Others are optical techniques measuring through skin, such as light scattering/occlusion, optical coherence tomography, or Raman spectroscopy of the upper layers of the skin (for a review of noninvasive glucose measurement techniques, see refs 4 and 5).

Among the optical techniques that can be used to analyze *in vitro* samples of blood or interstitial fluid, infrared (IR) spectroscopy in the mid-IR range is one of the most promising since it uses the vibrational modes of the glucose molecules that are highly specific and thus selective for glucose-sensing even in a complex matrix like full blood. Using infrared spectroscopy, the quantitative determination of glucose in samples of full blood, blood plasma, and dialysis fluid has been reported by many authors.[6−11]

The basis for the precise quantitative determination of body fluid constituents by mid-IR spectroscopy is the characteristic absorption of vibrational modes of the respective molecules. In the case of glucose, these are mainly the C−O−H stretching and bending vibrational modes in the so-called fingerprint region between approximately 800 and 1200 cm^{-1}. Because of

Received: September 30, 2012
Accepted: December 7, 2012
Published: December 7, 2012

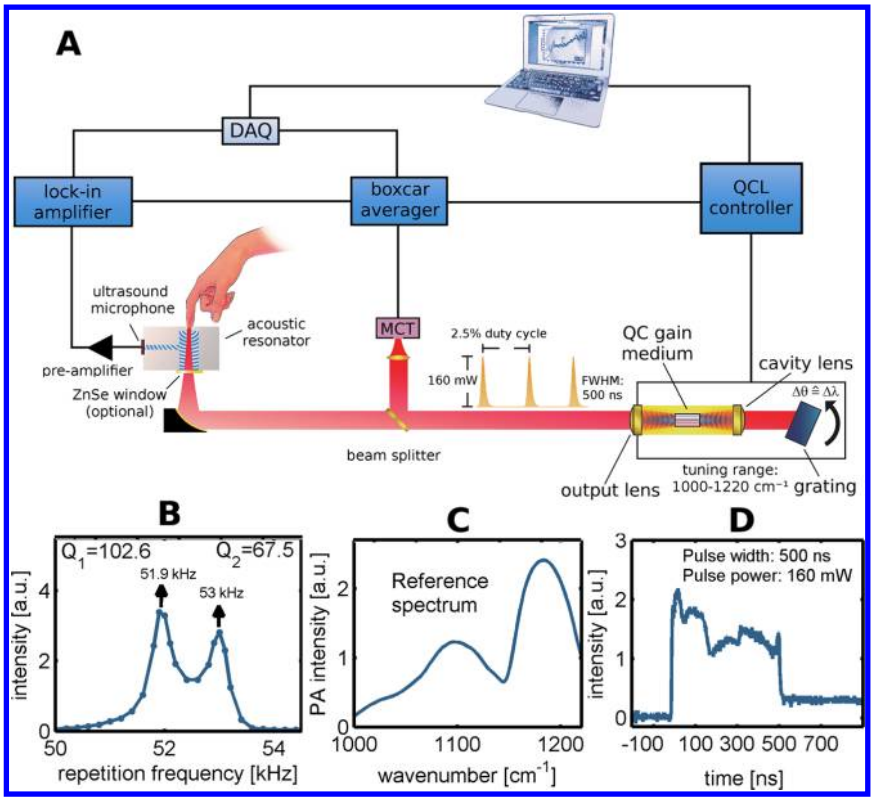

Figure 1. (A) Optical setup and schematic signal processing for the photoacoustic measurement of skin glucose. (B) Resonance profile of the photoacoustic cell measured with different repetition frequencies of the laser. The quality factors are indicated. (C) Photoacoustic spectrum of a carbon black broadband absorber, representing the laser's emission profile. (D) EC-QCL's pulse shape at maximum intensity of emission at 1170 cm^{-1}.

the overlap of absorption contributions from different blood constituents, multivariate analysis techniques such as partial least-squares (PLS) regression or principal component regression (PCR) are required; a conventional chemical/biochemical laboratory reference is used to establish a calibration matrix. The precision of these spectroscopic analysis techniques is high, approximately ±7 mg/dL in the case of glucose analysis in full blood samples,[9,12] and thus close to that of the most advanced laboratory techniques. However, they cannot be easily transferred to a noninvasive mode because of the low penetration depth of IR radiation in skin which is a consequence of the strong absorption by water O−H stretching and bending modes.

Interstitial fluid is the body fluid closest to the skin surface with a glucose content presumed to be relevant for blood glucose. Other body fluids are easily accessible, such as saliva, tear liquid, or urine but show either no correlation with blood glucose (such as urine, which contains glucose only in serious diabetes cases if the renal threshold is exceeded) or exhibit a long delay with respect to the increase or decrease of blood glucose (in the case of tears, this delay can be some hours). Furthermore, interstitial fluid represents a much simpler matrix than blood, without cellular components and mainly consisting of albumin and glucose, with traces of lactate.[13] Interstitial fluid is found in the *Stratum spinosum* layer located at a minimum depth of about 15−20 μm in skin, below the surface of the *Stratum corneum* layer. IR spectroscopy of interstitial fluid *in vivo* thus requires methods to detect the specific absorption of glucose in the *Stratum spinosum* layer.

In order to overcome the limitations of conventional IR spectroscopy for measuring opaque samples, like skin, and at the same time take advantage of the highly specific absorption bands of glucose in this spectral range, several authors have proposed the use of laser photoacoustic (PA) spectroscopy or photothermal radiometry using as sensors either piezoelectric transducers, a microphone in a gas cell, or an IR detector in the case of photothermal radiometry.[14−20] The photoacoustic studies involved the use of continuous wave (CW) or pulsed lasers with repetition frequencies in the audio range. Taking advantage of the high energy density offered by quantum cascade lasers (QCL), information on the absorption properties of glucose-containing skin phantoms and *in vivo* have been obtained.[13,21] A serious drawback of these approaches was (i) the use of individual (at most 2−3) IR wavelengths which does not allow one to take into account the variability of the background absorption of other skin components and of water, (ii) the long integration time required to compensate the low signal-to-noise ratio, and (iii) the interference of the surrounding acoustic noise. Any *in vivo* photoacoustic measurement on the skin taking more than some seconds is subject to fluctuations in the local body temperature, the pressure change due to pulsation or small movements, and the humidity on the skin or inside the PA-cell due to transpiration.

In order to overcome these problems, we have used a pulsed external cavity QCL (EC-QCL) laser system that can be tuned from approximately 1000 to 1220 cm^{-1}, i.e., across the glucose fingerprint region. We have combined this pulsed excitation with a photoacoustic cell designed for the ultrasound (US) range up to approximately 50 kHz. This combination allows us to operate the pulsed QCL at high repetition rates, which leads to higher energy deposition in the skin and reduces the perturbations by acoustic noise upon the *in vivo* measurement.

dx.doi.org/10.1021/ac302841f | *Anal. Chem.* 2013, 85, 1013−1020

This approach yields sufficient sensitivity to detect the small contribution of skin glucose to the total absorption of IR radiation in skin. Furthermore, the rapid scanning of the wavelength across the glucose fingerprint range (one spectrum every 15 s) warrants sufficient selectivity due to the use of glucose-relevant and glucose-invariant IR wavelengths in a rather short time.

We present here the *in vivo* absorption spectra between 1000 and 1220 cm^{-1} of the first three layers of human epidermis (*S. corneum*, *S. granulosum*, and *S. spinosum*) by photoacoustic spectroscopy. The glucose content in these layers is calculated by multivariate analysis including the entire measured wavelength range. The variation of the glucose concentration in these layers, and in particular in the *S. spinosum* layer where the glucose level rapidly adapts to the blood glucose level, is measured over the time during oral glucose uptake and metabolization in the standard oral glucose tolerance test (OGTT). The data demonstrate that, on the basis of mid-IR spectroscopy, a reliable and highly selective noninvasive glucose monitoring for diabetes patients could be performed.

EXPERIMENTAL SECTION

Optical Setup and Signal Processing. The optical setup and the signal processing developed for the photoacoustic measuring of glucose in skin is shown in Figure 1A. The collimated near-Gaussian profile laser beam from a tunable external cavity quantum cascade laser (EC-QCL Über Tuner 9, Daylight Solutions, California) is focused into the photoacoustic cell, with the focal plane at the contact surface to the skin, by an off-axis paraboloidal mirror forming a spot <1 mm in diameter on the skin. The external cavity laser has a tuning range between 1000 and 1220 cm^{-1} with a maximum pulse output power of 160 mW at 1170 cm^{-1}; for all the experiments described here the pulse width of the laser was kept at 500 ns.

The details on the mechanical design of the photoacoustic gas cell will be published elsewhere. Briefly, it consists of a T-shaped resonator with two cylindrical cavities perpendicularly connected, the absorption and the resonance cavity. The absorption cavity can be closed at one end by an antireflection-coated ZnSe window leaving the second end open to place either a reference sample or the skin, while an ultrasound microphone sensor (Knowles SPM0404UD5, Illinois) is placed at the end of the resonance cavity. The amplitude of the acoustic pulse in skin generated by the absorption of the laser pulse is coupled to the air in the photoacoustic cell and amplified by matching the laser repetition rate to 52 kHz, close to the cell resonance in the fifth harmonic mode determined as 51.9 kHz and with a quality factor Q (peak frequency/bandwidth) of 102 (Figure 1B).

The electrical signal measured by the ultrasound microphone sensor is further amplified and filtered by a lock-in amplifier (Stanford Research Systems SR810, Stanford) using a low pass time constant of 300 ms. A data acquisition system (National Instruments USB-9239) collects and transfers the DC signal from the lock-in amplifier to a personal computer. A full wavelength range scan of the quantum cascade laser was performed every 15 s, and up to 20 spectra were averaged to form a measuring point for the OGTT.

Figure 1C shows the emission spectrum of the laser in the range from 1000 cm^{-1} to 1220 cm^{-1}. This single-beam spectrum was obtained by placing on the open end of the photoacoustic cell a piece of black carbon material (SPI Glass 25, SPI Supplies, West Chester, Pennsylvania) which acts as a homogeneous broadband absorber. The glassy carbon black is considered to absorb 100% of the laser energy in the full range of the laser emission; thus, its photoacoustic signal represents the emission energy profile of the laser.[22,23] Single-beam spectra obtained with this carbon black reference were also used to calculate absorbance spectra for the skin.

The precision of the tuning range and the wavelength setting of the EC-QCL were controlled by measuring the photoacoustic spectra of a polyethylene naphthalate film, comparing these PA spectra with its absorption or transmission spectra measured by FT-IR spectroscopy.

A beam splitter (BS) was used to pass the major part of the IR energy to the photoacoustic cell (PA) and to reflect a smaller fraction to a thermoelectrically cooled mercury cadmium telluride (MCT) reference detector (HPC-2TE-100, Daylight Solutions, California). This detector is used to monitor the optical pulse and eventually correct for pulse-to-pulse fluctuations of the amplitude. Figure 1D shows the time course of the pulse intensity for the IR laser tuned to 1170 cm^{-1}. On the basis of the emitted laser peak power, pulse profile, pulse length, and repetition rate as well as on the losses due to beam splitter and cell entry window, care was taken that the irradiance of the skin was kept below 1 mW/mm^2 as required by radiation protection laws.[24]

***In Vivo* Measurements.** Preliminary photoacoustic measurements *in vivo* were carried out on healthy volunteers and on volunteers suffering from diabetes mellitus. A full study on a group of diabetes mellitus patients and a reference group of healthy volunteers approved by the ethics commission will be reported elsewhere. The hypothenar of the hand was selected as the location to place the photoacoustic cell. This location exhibits a rapid exchange of glucose between the blood and the interstitial fluid, thus reducing the time lag between blood and interstitial fluid glucose values. However, for comparison the photoacoustic spectra of different body positions were measured as well. In order to obtain the photoacoustic spectra of skin, the ratio of the respective signals with the photoacoustic signal of carbon black was formed, measured in the same spectral range and for identical laser and detection settings. No specific preparation of the skin was performed before the measurement.

Monitoring of the Glucose Level in Blood. The blood glucose level of the volunteers was measured every 5 min by a standard enzymatic test strip device (Bayer Contour Link Glucometer with Bayer Contour Sensors, Bayer Consumer AG, Basel, Switzerland). The standard procedure (pricking the finger tip, producing a drop of blood, transfer of this drop to the enzyme test stick, measurement) was applied as reproducible as possible. The precision and the repeatability of this combination of sensor and test strips are in agreement with the requirements of the DIN EN ISO 15197 standard for the CE (Conformité Européenne) label: 100% of the measured values with a real blood glucose above 75 mg/dL are in a ±20% range, and 100% of the values below 75 mg/dL are in a ±15 mg/dL range.[25] In some cases, a continuously measuring subcutaneous sensor device was used (DEXCOM SEVEN PLUS, DexCom Inc., San Diego, CA). This sensor is placed in the fat tissue of the abdominal wall and thus measures tissue glucose rather than blood glucose.

Variation of the Glucose Level. The glucose concentration in blood was modulated for healthy and diabetic volunteers using a standard oral glucose tolerance test (OGTT). In this test, starting from normal blood glucose

dx.doi.org/10.1021/ac302841f | *Anal. Chem.* 2013, 85, 1013−1020

values of approximately 90−110 mg/dL, the instant oral intake of glucose (75 g of glucose in 300 mL of water) leads to an increase of the blood glucose level over approximately 1 h to values >200 mg/dL with a subsequent decrease to normal values over 2−3 h. For diabetes patients, the OGTT leads to higher hyperglycemia and to a slower decrease to normal values; in this case we divided the glucose solution in two equal parts giving the first part at the beginning of the OGTT and the second part 80 min later. Low glucose levels (50−90 mg/dL) were recorded from volunteer diabetic patients reporting hypoglycemia.

FT-IR Spectroscopy. Infrared absorption spectra of the *S. corneum* and other components of the human epidermis like albumin and water were obtained using attenuated total reflection (ATR) spectroscopy on an FT-IR spectrometer (Bruker Vector 22, Bruker Optics, Ettlingen, Germany). The penetration depth of the IR beam into skin for the home-built ATR setup was estimated to be around 2−3 μm.

Multivariate Analysis. One of the most important advantages of measuring a full range spectrum in the glucose fingerprint region is the possibility of using multivariate analysis. In this case, principal component analysis and partial least-squares regression were applied to establish and validate the glucose prediction model for every measurement. The principal component analysis and the leave-one-out cross validation performed to the measured spectra sets were carried out using the PLS toolbox for MATLAB V7.1.0.246 (R14), Mathworks, Natick, MA.

RESULTS AND DISCUSSION

Spectral Features of Skin. Figure 2 shows a cross section of the human skin obtained from a histologic preparation. The

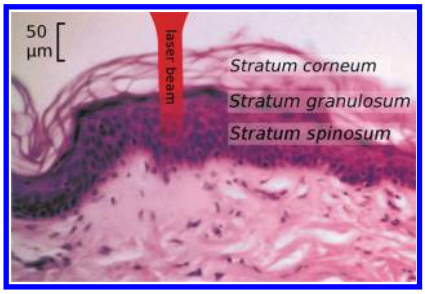

Figure 2. Layers of the human epidermal skin with a scheme of the laser beam visualizing the penetration depth of the laser through the layers.

S. corneum, *S. granulosum*, and *S. spinosum* layer can be clearly discerned. Although the thickness of the *S. corneum* is somehow variable, the interstitial fluid is typically found from a depth between 20 and 25 μm in the region of the *S. spinosum* layer. The *S. corneum* is the first epidermal layer that the laser irradiates. This relatively thin layer of about 15−20 μm thickness is an arrangement of corneocytes in a matrix of lipids and its main function is to act as a protection barrier against the intrusion of potentially dangerous agents to the human body and to prevent desiccation.[25−27] The *S. corneum* thickness represents more than 50% of the expected penetration depth of the laser radiation in skin. It is thus expected that the absorption spectra of skin measured in the range from 1000 to 1220 cm^{-1} are dominated by the absorption properties of keratin and the lipids that form the *S. corneum*.

Figure 3 shows a photoacoustic spectrum of skin taken at the left hypothenar of the hand of a volunteer in the hypoglycemic

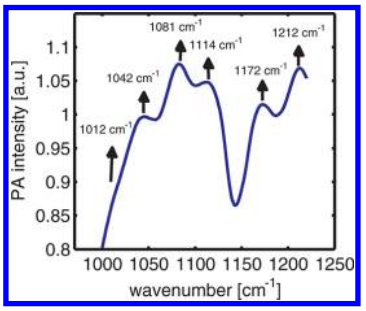

Figure 3. Photoacoustic spectrum of human skin in the glucose fingerprint region between 1000 and 1220 cm^{-1}. The major peak frequencies correspond to the lipid layers and corneocytes.

state, with a blood glucose concentration lower than 50 mg/dL. The intensity of the PA signals corresponds to the absorption strength; positive bands in the PA spectrum are thus related to absorbance bands in an optically recorded IR spectrum. The spectrum is dominated by the PO_2^- symmetric stretching vibration close to 1080 cm^{-1}, the C−O−P stretching vibration at about 1042 cm^{-1}, a band close to 1172 cm^{-1} assigned to the ester C═O stretching mode, and a band at 1210 cm^{-1} which can be assigned to the PO_2^- antisymmetric stretching mode. The band at 1116 cm^{-1} could be due to the υ(CC) found for trans lipids. The vibrational modes in the measured spectral range are characteristic for carbohydrated lipids, nucleic acids, and proteins, and their exact positions depend on factors like temperature and hydration.[28−30]

For the *S. granulosum* and *S. spinosum* layers, the amount of lipids is expected to be lower than that for the *S. corneum*. The main contribution of these layers to the spectra arises from the keratin in the keratinocyte and from the glucose and albumin found in the *S. spinosum*. The photoacoustic spectra measured for different positions on the skin, with different thickness of the *S. corneum* and different content of lipids, should thus reflect this composition by changing band positions and band intensities. Figure 4 shows the photoacoustic spectra of different parts of the skin: wrist, hypothenar, fingertip, and thenar. For comparison, the attenuated total reflection (ATR) spectrum of the fingertip is shown. All photoacoustic spectra represent the integral absorption of IR radiation over the entire depth of the layer from the skin surface (d = 0) to approximately d = 40−50 μm. In contrast, the ATR spectrum of the fingertip (lowest trace) represents only about 3 μm of absorbing layers.

The absorption peaks observed in the PA spectra measured at different skin locations slightly differ in the positions and relative intensities of the absorption bands due to different lipid and corneocytes content and different *S. corneum* thickness. For those sites where the *S. corneum* is expected to be thinner (such as the wrist and the thenar), the absorption band for the keratinocytes at 1080 cm^{-1} is more pronounced than the others due to the reduction of the contribution from the lipid matrix. The main spectral features of the photoacoustic spectra measured in skin are in good agreement with the spectra for *S. corneum* measured by FT-IR spectroscopy, which confirms the dominant absorbance from the *S. corneum*.[31−35]

Water is typically a problem in the IR spectroscopy of biological material due to the O−H stretching and bending

dx.doi.org/10.1021/ac302841f | *Anal. Chem.* 2013, 85, 1013−1020

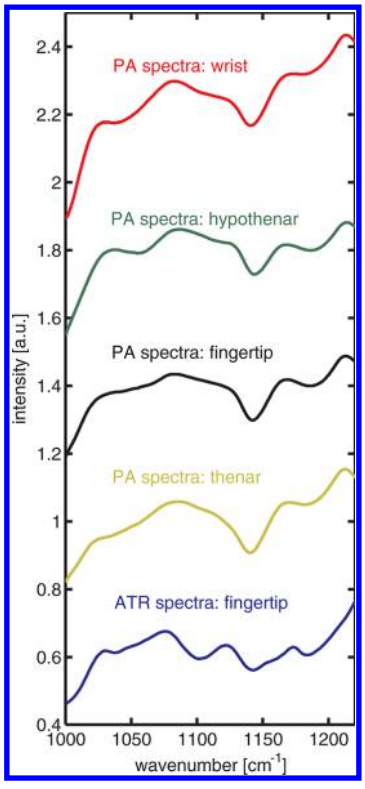

Figure 4. Photoacoustic spectra of human skin at different positions. The spectra are vertically shifted for better discrimination. The lowest trace shows an ATR spectrum of the fingertip for comparison (absorption scaled to fit PA spectra).

modes as well as due to the broad absorption background arising from hydrogen bonded structures. However, in the photoacoustic spectra presented here as well as in the ATR spectrum, the water background did not present a problem. This is due to the low percentage of water content found in the epidermis (about 20% and even lower in the *S. corneum*).[31]

Photoacoustic Spectra of the Epidermis upon Changing Blood Glucose Concentration. In order to analyze the influence of variable skin glucose on the PA spectra, the left hypothenar of a diabetic volunteer was kept fixed on the PA cell and a series of photoacoustic spectra of the epidermis, such as the one shown in Figure 3, were measured while the concentration of glucose in blood changed from 37 to 237 mg/dL over a period of 175 min. The volunteer, a type-I diabetes patient who had agreed to perform an oral glucose tolerance test (OGTT), had reported hypoglycemia; when the test started he measured a blood glucose value of 56 mg/dL and reached the minimum value of 37 mg/dL five minutes after the start of the test. When the minimum glucose value was reached, the uptake of glucose was initiated through oral administration of glucose by the volunteer. Consequently, the glucose level increased and reached the maximum value after approximately 170 min.

Since the lipid-corneocytes configuration of the *S. corneum* is not expected to change during the rather short time of the test, the main spectral features changing with the blood glucose should come from the glucose in the interstitial fluid found in the *S. spinosum.* This is expected because glucose metabolism is a much faster process than any other metabolic process in the epidermis. This can be observed in the difference PA spectra of skin during the test if the photoacoustic spectrum at the hypoglycemic state (i.e., with the lowest glucose level) is taken as a reference and subtracted from the rest in order to eliminate the spectral features of the matrix. Figure 5 shows some

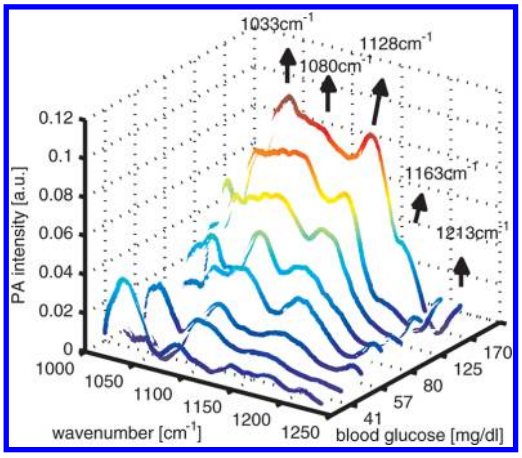

Figure 5. Variation of the photoacoustic spectra of a diabetic volunteer during an OGTT, where the blood glucose rose from 37 to 237 mg/dL. The spectrum corresponding to the lowest blood glucose value was subtracted to correct for the background matrix. The absorption features of glucose can be observed as the glucose concentration in blood increases.

relevant difference spectra for different blood glucose concentrations. In this figure, the well-known spectral features of glucose appearing at 1033, 1077, 1128, 1163, and 1213 cm^{-1} can be observed while the glucose concentration in blood is increasing.

Principal Components of the Photoacoustic Spectra of the Skin. The assumption of an invariant background due to the matrix absorbance, as explained in the last section, may be only partly justified; it could apply just to the lipid and keratinocyte absorbance. However, during an OGTT, hydration of the *S. corneum* may vary, thus leading to additional variable contributions on top of the contributions due to glucose change.

Because of the spectral and time resolution obtained with the combination of the EC-QCL and ultrasound PA detection described here, the common features of the PA spectra obtained in the course of glucose variation from low to high values can be analyzed by principal component analysis (PCA). Applying this multivariate analysis to the spectra shown in Figure 5 leads to the identification of three major components that altogether represent more than 93% of the variations in the PA signal.

The dominant component (PC1) in the PA spectra representing approximately 72% fits well to the absorption spectrum of glucose, and its behavior during the OGTT follows the blood glucose time course as show in Figure 6A. At this point it is important to note that, in a principal component analysis, the algorithm applied does not require any input of the glucose level of the sample. Therefore, it can be considered as a blind test for the correlation of the photoacoustic intensity change vs the change of glucose in the sample.

The second most relevant component (PC2) in the PA spectra, Figure 6B, which amounts to approximately 16% exhibits a smooth rise from 1000 to >1200 cm^{-1} with only very little structure. We propose that PC2 represents water absorbance in the *S. corneum*. In the specific situation of the OGTT's performed here, the photoacoustic cell was in

dx.doi.org/10.1021/ac302841f | *Anal. Chem.* 2013, 85, 1013−1020

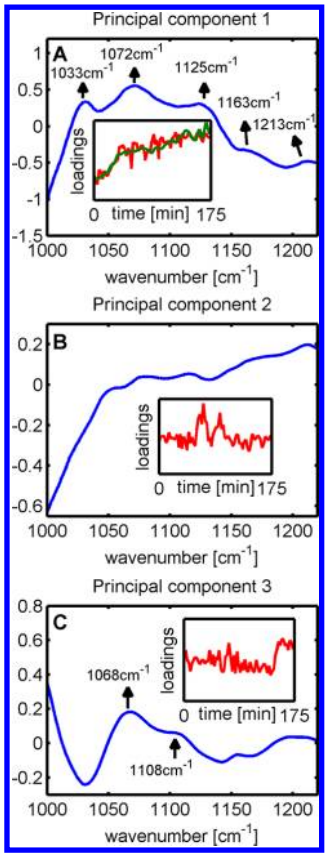

Figure 6. The first three principal components of the PA signal variation after background correction and their main peaks are shown in parts A–C. The scores are shown in blue, while the loadings are marked red. (A) The scores of the first PC correspond with the glucose absorption spectrum. In the inside box the loadings (red) are compared to measured blood glucose (green). (B) The second component corresponds with the spectrum of water. (C) The third component shows two peaks which are in agreement with the absorbance of phosphate.

permanent contact with the skin. This did not allow the target part of the skin to equilibrate with the low relative humidity in the laboratory and, therefore, some water condensation might have occurred on the sample surface or atop the PA-cell window.

Finally, PC3 (Figure 6C) accounts for approximately 5.6% of the variation, and exhibits spectral features that resemble the phosphate PO modes. At present, we have no consistent interpretation for the molecular basis of this PO absorbance in skin. It is clear that this "phosphate-like" spectral feature that appears close to the end of the OGTT, when the blood glucose concentration is higher than 200 mg/dL, does not arise as an additional component but rather replaces in part glucose absorbance. One possible explanation could be phosphorylation of glucose which, however, would involve hexokinase as an enzyme.[36] This process is known in glucose metabolism for the preparation of glycolysis, and it has been observed in the epidermis but only *in vitro*.[37,38]

Invasive vs Noninvasive Measurements of Glucose during Oral Glucose Tolerance Tests. In order to validate the determination of glucose level by noninvasive PA measurement, we have performed a series of OGTTs on healthy and diabetic volunteers. As a reference, the blood glucose level was determined by test strip systems every 5 min using a drop of blood from the finger tip. In addition, one of the volunteers, a type I diabetes patient, used a subcutaneous sensor in the fat tissue for continuous measurement. The results of the leave-one-out cross validations of the partial-least-squares regression applied to this series of OGTTs are shown in Figure 7.

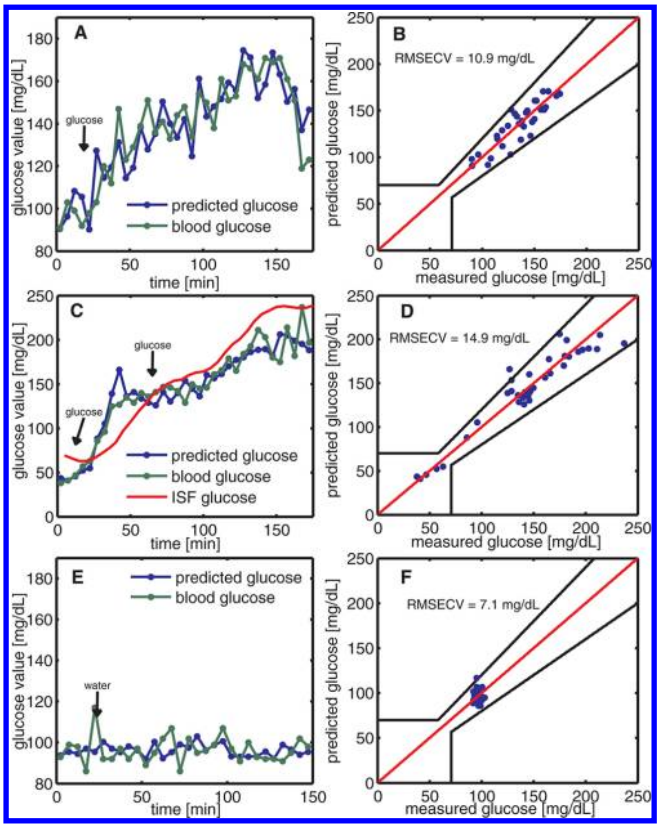

Figure 7. Examples for parallel invasive/noninvasive glucose measurements during an OGTT. (A,B) OGTT was conducted on a healthy person. (A) Time course of blood glucose measured by enzymatic test strips and noninvasively by photoacoustic spectroscopy. (B) Correlation between measured blood glucose and predicted glucose. Clarke's error grid is shown. (C,D) OGTT was conducted on a diabetic patient. (C) Time course of blood glucose measured by enzymatic test strips, ISF glucose in subcutaneous fat tissue measured by a sensor tip, and noninvasive measurement by photoacoustic spectroscopy. In contrast to subcutaneous ISF measurement, no time delay was found between blood glucose and epidermal glucose measured by PA spectroscopy. (D) Correlation between measured blood glucose and predicted glucose. Clarke's error grid is shown. (E,F) Control measurement where no glucose was consumed but the same volume of water. (E) Time course of blood glucose measured by enzymatic test strips and noninvasively by PA spectroscopy. (F) Correlation between measured blood glucose and predicted glucose. Clarke's error grid is shown.

Figure 7A shows the time course of the glucose level as measured every 5 min noninvasively and by the test strip system for a healthy volunteer. After glucose administration as indicated by the arrow, the level of blood and of interstitial glucose rose from the initial value of approximately 90–100 mg/dL to approximately 170–180 mg/dL over 2 h and then decayed to the starting value. The different methods of glucose analysis, invasive and noninvasive, yield similar glucose concentrations over the time of the OGTT and both follow exactly the same time course. The correlation between the

dx.doi.org/10.1021/ac302841f | *Anal. Chem.* 2013, 85, 1013–1020

invasive and the noninvasive glucose measurement is shown in Figure 7B. The mean prediction error calculated from this correlation is approximately 11 mg/dL. We would like to emphasize that this error is partly due to the reference method used and could be significantly improved if a clinical laboratory reference could be used. At this stage of the studies, however, we refrain from taking this reference method since it would require a much larger amount of venous blood taken every 5 min from the volunteer.

Figure 7C shows the time course of the glucose level as measured every 5 min noninvasively as well as by the test strip system and by a subcutaneous sensor in the abdominal wall for a type I diabetes volunteer. In this case, the volunteer started in a hypoglycemic state. The glucose level increased rapidly to values between 120 and 140 mg/dL and further over the next 2 h and finally reached values above 200 mg/dL, persisting much longer than for a healthy person. As in Figure 7A, the different methods of glucose determination yield similar glucose concentrations over the time of the OGTT, although the lag of the glucose concentration measured by the subcutaneous sensor in the fat tissue is evident. This can be explained by the slow equilibration of blood glucose and tissue glucose in this skin region. There is also an interesting overshoot in the time course observed with the photoacoustic sensor indicating a rapid transient increase in skin glucose. The correlation between the blood glucose and the epidermal glucose concentration measured by the noninvasive photoacoustic method is shown in Figure 7D. The mean prediction error calculated from this correlation is approximately 15 mg/dL.

In addition to the OGTT carried out for the healthy and diabetic patient, we tested the selectivity and specificity of our approach by measuring the PA spectra of a healthy patient during a nonglucose changing situation. In this case, the PA measurements were conducted just like for the OGTTs shown in Figure 7A,C, but instead of drinking a glucose solution the patient took 300 mL of water. The results of this test are shown in Figure 7E,F indicating that the system provides enough selectivity to represent changes exclusively arising from the modulation of the glucose concentration in the epidermis.

The correlation diagrams in Figure 7B,D,F also contain lines that are termed the Clarke Error Grid Analysis.[39] This method is used to determine the accuracy of blood glucose measuring methods and defines regions of sufficient accuracy as well as regions of low accuracy, but without negative consequence and inaccurate treatment for the patient. We would like to emphasize that all data points fall within the critical lines of the Clarke error grid, which would be the requirement for a clinical use of this method.

The principal components analysis of the photoacoustic spectra, explained in the last section, shows that there are several parameters that can eventually produce interference when calculating the glucose content in the samples; change in the PA sensor sensitivity, water condensation in the window or in the sample, changes in the configuration of the lipid layer due to temperature or humidity, etc. However, by applying a multivariate calibration, the selectivity and specificity of the measurement system presented in this work, supported by Figure 7, allow the determination of the glucose concentration behavior in the interstitial fluid.

CONCLUSIONS AND OUTLOOK

We have demonstrated here the feasibility of *in vivo* noninvasive spectroscopy of the skin layers that contain glucose in a concentration comparable to blood glucose. This could be achieved by combining PA spectroscopy and a pulsed EC-QCL that can be tuned across a wavelength range in the fingerprint region which is highly selective for glucose but also contains bands from lipids and keratin. Experimentally, the use of a PA cell optimized for the ultrasound range has led to a signal-to-noise ratio that now permits the use of this measurement system for noninvasive glucose monitoring.

The IR spectra of skin obtained are complex but can be separated into principal components thanks to the tunability of the laser. They represent to a large extent the uppermost skin layer *S. corneum* and to a smaller extent the *S. granulosum* and the *S. spinosum* layers. The fact that glucose is found to be the first principal component is a good indicator of the robust measurement that can be achieved by the PA approach. Furthermore, we have also shown that multivariate data analysis is able to separate the variations of glucose from changes of humidity of the skin or other metabolic components in the sample. We also should consider further interfering substances such as medically relevant drugs and cosmetics.

Since the incidence of the laser energy is below 1 mW/mm^2 and does not hurt, dry, or alter the skin, this PA spectroscopy of the glucose-containing skin layers represents a true noninvasive glucose monitoring. As demonstrated with the preliminary results shown here, it is sensitive enough to continuously follow the changes of the glucose level of a diabetes patient and it is highly selective to discern glucose from other constituents of the interstitial fluid. These properties would lead to positive secondary effects in that the dangerous extreme variations of glucose (the highs and lows) could be avoided. For instance, they could form the basis to establish the so-called artificial pancreas for type I diabetes patients. A potential concern might be the patient-to-patient correlation due to the different skin properties of different patients. Variations of the thickness of the *Stratum corneum* layer, for instance, could affect the signal amplitude, and therefore, an individual calibration for each patient might be required.

AUTHOR INFORMATION

Corresponding Author

*E-mail: maentele@biophysik.uni-frankfurt.de.

Notes

The authors declare no competing financial interest.

ACKNOWLEDGMENTS

The authors would like to thank Ernst Winter and Andreas Roth (Institut für Biophysik) for the excellent mechanical and electronic engineering. Miguel A. Pleitez would like to acknowledge the Deutscher Akademischer Austauschdienst (DAAD) for a Ph.D. fellowship and to the University of El Salvador for supporting his studies in Germany.

REFERENCES

(1) Scully, T. *Nature* **2012**, *485*, S2−S3.
(2) Kuo, C.-Y.; Hsu, C.-T.; Ho, C.-S.; Su, T.-E.; Wu, M.-H.; Wang, C.-J. *Diabetes Technol. Ther.* **2011**, *13*, 596−600.
(3) Alto, W. A.; Meyer, D.; Schneid, J.; Bryson, P.; Kindig, J. *J. Am. Board Family Pract./Am. Board Family Pract.* **1997**, *15*, 1−6.
(4) Oliver, N. S.; Toumazou, C.; Cass, A. E. G.; Johnston, D. G. *Diabetic Med.* **2009**, *26*, 197−210.
(5) Ciudin, A.; Hernandez, C.; Simo, R. *Curr. Diabetes Rev.* **2012**, *8*, 48−54.

(6) Roth, A.; Dornuf, F.; Klein, O.; Schneditz, D.; Hafner-Gießauf, H.; Mäntele, W. *Anal. Bioanal. Chem.* **2012**, *403*, 391−399.
(7) Damm, U.; Kondepati, V. R.; Heise, H. M. *Vib. Spectrosc.* **2007**, *43*, 184−192.
(8) Heise, H. M.; Damm, U.; Bodenlenz, M.; Kondepati, V. R.; Köhler, G.; Ellmerer, M. *J. Biomed. Opt.* **2007**, *12*, 024004-1−024004-12.
(9) Hoşafçi, G.; Klein, O.; Oremek, G.; Mäntele, W. *Anal. Bioanal. Chem.* **2007**, *387*, 1815−1822.
(10) Vrančić, C.; Fomichova, A.; Gretz, N.; Herrmann, C.; Neudecker, S.; Pucci, A.; Petrich, W. *Analyst* **2011**, *136*, 1192−1198.
(11) Spanner, G.; Niessner, R. *Fresenius J. Anal. Chem.* **1996**, *354*, 306−310.
(12) Bhandare, P.; Mendelson, Y.; Peura, R. A.; Janatsch, G.; Kruse-Jarres, J. D.; Marbach, R.; Heise, H. M. *Appl. Spectrosc.* **1993**, *47*, 1214−1221.
(13) Pleitez Rafael, M. Á.; Von Lilienfeld-Toal, H.; Mäntele, W. *Spectrochim. Acta Part A: Mol. Biomol. Spectrosc.* **2011**, *85*, 61−65.
(14) Christison, G. B.; MacKenzie, H. A. *Med. Biol. Eng. Comput.* **1993**, *31*, 284−290.
(15) von Lilienfeld-Toal, H.; Weidenmüller, M.; Xhelaj, A.; Mäntele, W. *Vib. Spectrosc.* **2005**, *38*, 209−215.
(16) Myllylä, R.; Zhao, Z.; Kinnunen, M. In *Handbook of Optical Sensing of Glucose in Biological Fluids and Tissues Series in Medical Physics and Biomedical Engineering*; Tuchin, V. V., Ed.; Taylor & Francis Group: Boca Raton, FL, 2009; pp 419−455.
(17) MacKenzie, H. A.; Ashton, H. S.; Spiers, S.; Shen, Y.; Freeborn, S. S.; Hannigan, J.; Lindberg, J.; Rae, P. *Clin. Chem.* **1999**, *45*, 1587−1595.
(18) Kottmann, J.; Rey, J. M.; Sigrist, M. W. *Rev. Sci. Instrum.* **2011**, *82*, 084903.
(19) Spanner, G.; Niessner, R. *Fresenius J. Anal. Chem.* **1996**, *355*, 327−328.
(20) Guo, X.; Mandelis, A.; Zinman, B. *Biomed. Opt. Express* **2012**, *3*, 3012−3021.
(21) Kottmann, J.; Rey, J. M.; Luginbühl, J.; Reichmann, E.; Sigrist, M. W. *Biomed. Opt. Express* **2012**, *3*, 667.
(22) Michaelian, K. H. *Photoacoustic Infrared Spectroscopy*; Wiley-Interscience: Hoboken, NJ, 2003.
(23) Dehghany, M.; Michaelian, K. H. *Rev. Sci. Instrum.* **2012**, *83*, 064901.
(24) Das Europäische Parlament und der Rat der Europäischen Union. *Richtlinie 2006/25/EG des Europäischen Parlaments und des Rates*; 2006; pp 38−59.
(25) Bouwstra, J. .; Honeywell-Nguyen, P. *Adv. Drug Delivery Rev.* **2002**, *54*, S41−S55.
(26) Bommannan, D.; Potts, R. O.; Guy, R. H. *J. Invest. Dermatol.* **1990**, *95*, 403−408.
(27) Downing, D. T. *J. Lipid Res.* **1992**, *33*, 301.
(28) Lewis, R. N. A. H.; McElhaney, R. N. In *Infrared Spectroscopy of Biomolecules*; Mantsch, H. H., Chapman, D., Eds.; Wiley-Liss: New York, 1996; pp 159−202.
(29) Jackson, M.; Mantsch, H. H. In *Infrared Spectroscopy of Biomolecules*; Mantsch, H. H., Chapman, D., Eds.; Wiley-Liss: New York, 1996; pp 311−340.
(30) Liquier, J.; Taillandier, E. In *Infrared Spectroscopy of Biomolecules*; Mantsch, H. H., Chapman, D., Eds.; Wiley-Liss: New York, 1996; pp 131−158.
(31) Greve, T. M.; Andersen, K. B.; Nielsen, O. F. *Spectroscopy* **2008**, *22*, 437−457.
(32) Laugel, C.; Yagoubi, N.; Baillet, A. *Chem. Phys. Lipids* **2005**, *135*, 55−68.
(33) Barry, B. W.; Edwards, H. G. M.; Williams, A. C. *J. Raman Spectrosc.* **1992**, *23*, 641−645.
(34) Garidel, P. *Phys. Chem. Chem. Phys.* **2002**, *4*, 5671−5677.
(35) Fabian, H.; Jackson, M.; Murphy, L.; Watson, P. H.; Fichtner, I.; Mantsch, H. H. *Biospectroscopy* **1995**, *1*, 37−45.
(36) Berg, J. M.; Tymoczko, J. L.; Stryer, L. In *Stryer Biochemie*; Spektrum Akademischer Verlag GmbH: Heidelberg, Germany, 2007; pp 484−530.
(37) Kenneth, H. M.; Ohkawara, A. *J. Invest. Dermatol.* **1966**, *46*, 278−282.
(38) Decker, R. H. *J. Invest. Dermatol.* **1971**, *57*, 351−363.
(39) Freckmann, G.; Baumstark, A.; Jendrike, N.; Zschornack, E.; Kocher, S.; Tshiananga, J.; Heister, F.; Haug, C. *Diabetes Technol. Ther.* **2010**, *12*, 221−231.